Control of Transformerless Inverter in Standalone Photovoltaic MPPT Systems

Ahmet Yuksel, Emre Ozkop

Department of Electrical and Electronics Engineering, Karadeniz Technical University, Turkey
ahmetyuksel@ktu.edu.tr, eozkop@ktu.edu.tr

Abstract

This paper presents the simulation performance of control of a standalone photovoltaic (PV) maximum power point tracking (MPPT) system with transformerless inverter. The tested control strategy for PV module is based on Perturb and Observe (P&O) MPPT algorithm, and current and voltage are employed to enhance controllability of the control scheme applied into a dc-dc boost type power converter. A single-phase HERIC (Highly Efficient and Reliable Inverter Concept) transformerless inverter connected as an output to the converter is applied and controlled to feed ac loads.

1. Introduction

Renewable energy is a one of the solutions and exit way where both electrical energy consumption has increased and conventional energy sources such as oil, gas and coal have run out day by day. On one hand, the conventional sources have caused some undesired circumstances such as environmental problems, concerns of people about energy sources yielding, conflict of interest of countries, etc. On the other hand, renewable energy sources have become a new hope to defeat these situations and make a contribution to provide energy supply & demand balance and enhance sustainability and reliability on grid electricity [1].

Renewable energy provided about 19% of global final energy consumption in 2015 and one of the types is a solar photovoltaic (PV). As solar PV capacity was 228 GW in 2015, this capacity increased in 2016 and reached 303 GW. Besides, more than 15 countries had enough solar PV capacity to provide 2% or more of their electricity demand during 2016 [2].

Basic solar PV system consists of PV modules, power electronic converters (dc-dc and dc-ac) and control mechanism for the converters to utilize the PV output power. Due to non-linear voltage-current characteristics of the PV modules and impacts of weather conditions on PV power generation, necessity of tracking of maximum power point of the PV arises to extract maximum power [3]. There are various maximum power point tracking (MPPT) algorithms in the literature and some of them such as Perturb and Observe (P&O), Incremental Conductance (INC), dp/di or dp/dv and optimization based methods that stands out where each of them has pros and cons that should be considered [4].

There are different topologies and structures for solar PV systems depending on applications. Especially, the power electronic converter topologies varieties according to load or consumer electricity consumption types (dc or ac) [5]. For example, an inverter (dc-ac converter) is necessary to supply AA loads and this inverter can be designed with or without transformer part [6]. In recent years, transformerless PV inverter topologies are more preferable since a transformer causes some unfavorable effects such as decreasing efficiency, and increasing cost and dimension in a transformer PV inverter [7].

Various transformerless PV inverter topologies and different classification perspectives are there and HERIC, H5, H6, Steca, NPC, ANPC and Conergy are some well-known of them in the literature [8, 9, 10]. Comparison between them can be done mainly in number of components, output voltage level, leakage current, efficiency, and etc [10]. For instance, while NPC, Conergy and Vincotech inverters have four switches, HERIC, H6, Steca and ANPC inverters consists of six of them. There is no direct connection between leakage current-efficiency and number of switches so that leakage current is lower level and efficiency about 97.67% in Conergy inverter whereas H5 inverter, which has five switches, has low leakage current and 98.5% efficiency [8].

Control of the transformerless PV inverters is based on measured current and voltage managements and different control methods are offered to extract maximum power, realize active-reactive power flow control for grid-connected applications, regulate a dc-bus voltage and provide desired power quality level to consumers, and etc. [11, 12, 13].

In this paper, a standalone photovoltaic MPPT system with transformerless inverter is designed, controlled and simulated. Perturb and Observe (P&O) algorithm is preferred to be applied with a dc-dc boost converter to track maximum power point. Single-phase HERIC transformerless inverter is considered to feed loads.

2. System Design

Architecture of the standalone photovoltaic (PV) MPPT systems with transformerless inverter is shown in Fig. 1. The system structure consists of photovoltaic nodules, dc-dc power converter, LC filter, transformerless inverter, LCL filter and load. Maximum power point tracking algorithm based on perturbation & observe structure is used to control output power of photovoltaic modules. The PV power transfers into transformerless inverter thorough the LC filter to eliminate ripples on voltage. DC voltage induced on the filter output is converted into ac voltage waveform by transformerless inverter and injected to the load through the LCL filter.

2.1. Maximum Power Point Tracking Algorithm

In this paper, the maximum power point tracking algorithm based on the Perturb and Observe (P&O) technique is illustrated in Fig. 2. The P&O technique is based on the perturbation voltage at regular intervals then comparing the power of the PV system output associated with the previous perturbation cycle. Power and voltage values are used for tracking the maximum power point of photovoltaic system. The measured voltage and current of PV system output are employed to acquire PV power as given below.

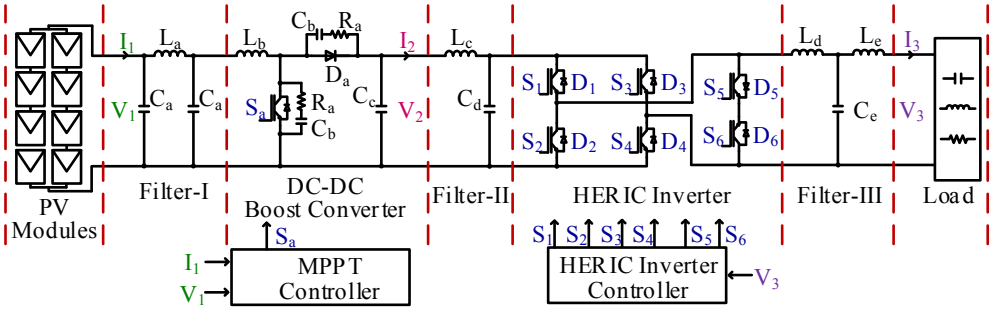

Fig. 1. Schematic for the simulation setup of the standalone photovoltaic MPPT system with the transformerless inverter

$$P_{PV}(k) = V_{PV}(k) \times I_{PV}(k) \quad (1)$$

where P_{PV}, V_{PV} and I_{PV} are power, voltage and current values of PV system output.

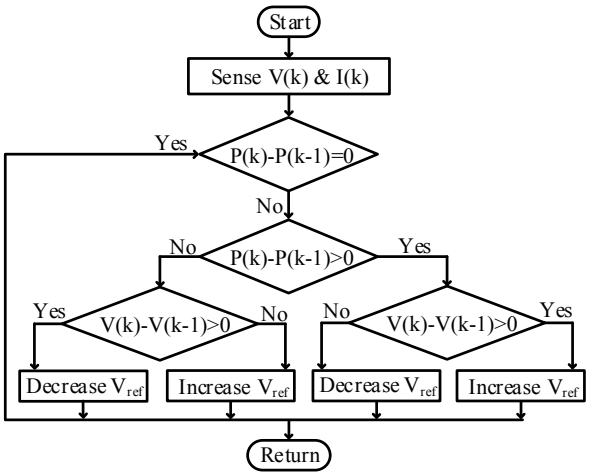

Fig. 2. Perturb and observe technique structure

The power variation ($\Delta P_{PV} = P_{PV}(k) - P_{PV}(k-1)$) and voltage variation ($\Delta V_{PV} = V_{PV}(k) - V_{PV}(k-1)$) determine the immediate operation point and requirement action with corresponding decrease or increase in the voltage. The possible scenarios related to the variations (ΔP_{PV} and ΔV_{PV}) can be summarized in table as given Table 1.

Table 1. The possible scenarios depends the variations

STATUS		ACTION
ΔP_{PV}	ΔV_{PV}	$V_{ref}(k)$
Positive	Positive	Increase
Positive	Negative	Decrease
Negative	Positive	Decrease
Negative	Negative	Increase
Zero	-	No

The action on voltage ($V_{ref}(k)$) is realized by changing the duty cycle of the pulse width modulation (PWM) signal of switch of dc-dc power converter in this study.

2.2. DC-DC Power Converter

There are various dc-dc power converter topologies in the literature and these topologies has pros and cons regarding to different angles such as size, weight, power, efficiency, and number of components, etc. One of the dc-dc power converter topologies is a boost converter and it consists of three passive and one active components as shown in Fig. 1.

2.3. Transformerless PV Inverter

HERIC (Highly Efficient and Reliable Inverter Concept) inverter is one of the transformerless PV inverter topologies. HERIC Inverter derived from the classical H-bridge topology by adding a bypass leg has six switches which of four are switched at high frequency and two are switched at grid frequency. The operation states of HERIC inverter are depicted in Fig. 3 and tabulated in Table 2.

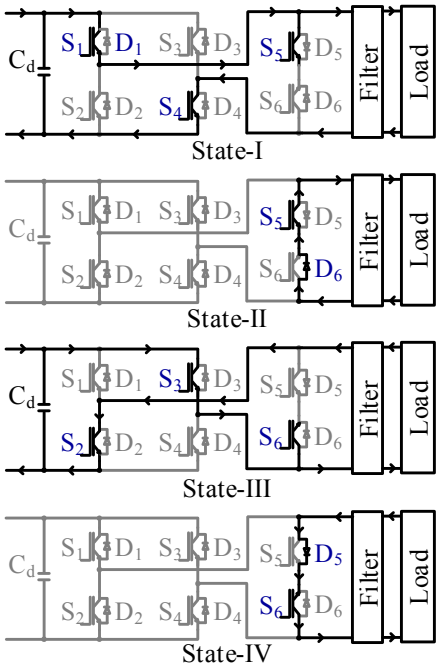

Fig. 3. The operation states of the HERIC inverter

Table 2. The switching states of the HERIC inverter

State	S_1	S_2	S_3	S_4	S_5	S_6	D_5	D_6	V_{output}
I	+	-	-	+	+	-	-	-	V_{PV}
II	-	-	-	-	+	-	-	+	0
III	-	+	+	-	-	+	-	-	$-V_{PV}$
IV	-	-	-	-	-	+	+	-	0

Not: "+" ON, "-" OFF

This topology provides many advantages such as lower core losses, higher efficiency due to no reactive power exchange between Filter-III and Filter-II during zero voltage and to lower frequency switching in one leg and very low leakage current and EMI, where S1, S2, S3 and S4 switches are switched at high frequency and S5 and S6 switches are switched at grid frequency as shown in Fig. 4.

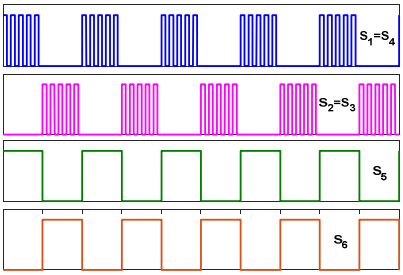

Fig. 4. The switching signals of the HERIC inverter

The LCL type filter is used for Filter-III and filter parameters are defined as follows by using Equations (2-4) [14-16].

$$L_d = L_e = \frac{V_3}{2\sqrt{6} \times i_{ripm} \times f_s} \quad (2)$$

$$f_{res} = \frac{1}{2\pi}\sqrt{\frac{L_d + L_e}{L_d \times L_e \times C_e}} \quad (3)$$

$$10f \leq f_{res} \leq 0.5f_s \quad (4)$$

where i_{ripm}, peak value of current harmonic, f_{res}, resonance frequency, f_s, switching frequency and f, grid frequency.

2.4. HERIC Inverter Controller

The single loop control structure is applied to control HERIC inverter. In the control structure, a classical PI controller is used to manage the inverter output voltage. Instantaneous output and reference (desired) voltages are inputs of the controller. The difference between voltages is named as an error in voltage and this error is sent to the PI controller. The value of the controller fed into the PWM generator to generate suitable switching signals for the switches.

3. Simulation

The standalone photovoltaic MPPT system with transformerless inverter is simulated by Matlab/Simulink environment. The system simulation parameters are given in Table 3.

The simulation results are shown in Figs. 5-8. In this simulation case, solar irradiation and ambient temperature, which are two important environmental factors effecting on efficiency of PV electric power generation, have patterns show in Fig. 5.

Before the system is powered, the PV array output can be characterized as a zero power-maximum voltage (open circuit voltage)-minimum current (zero current) behavior. When the standalone PV MPPT system with HERIC transformerless inverter is powered, power flow from PV side to load side. at the beginning, consumption in current increases, meanwhile voltage decrease due to nonlinearity of the power–voltage (P-V) and current-voltage (I-V) characteristic of PV arrays as observed in Fig. 6.

Table 3. The system simulation parameters

PV module		**dc-dc converter**		**Filter-I**	
V_{oc}	44.2 V	L_b	5 uH	L_a	124 uH
I_{sc}	7.62 A	R_a	33 Ohm	C_a	68 uF
N_{series}	6	C_b	300 pF	**Filter -II**	
$N_{parallel}$	6	C_c	2 mF	L_c	5.2 uH
		f_s	1 kHz	C_d	2 mF
HERIC PI controller				**Filter -III**	
K_P	10	K_I	5	L_d	40 mH
f_s	1 kHz	K_D	0.05	L_e	40 mH
P&O MPPT technique				C_e	0.65 mF
D_{max}	0.8	$D_{initial}$	0.5	**Load**	
D_{min}	0.4	ΔD	30u	P	7.5 kW
Not: Duty cycle: D				f	50 Hz

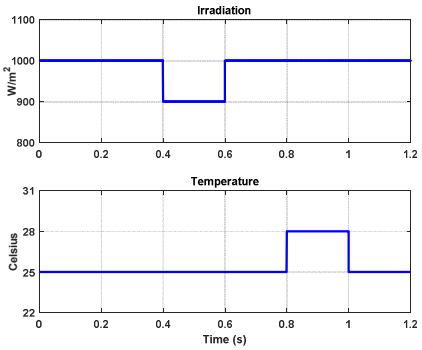

Fig. 5. The photovoltaic system irradiation and temperature

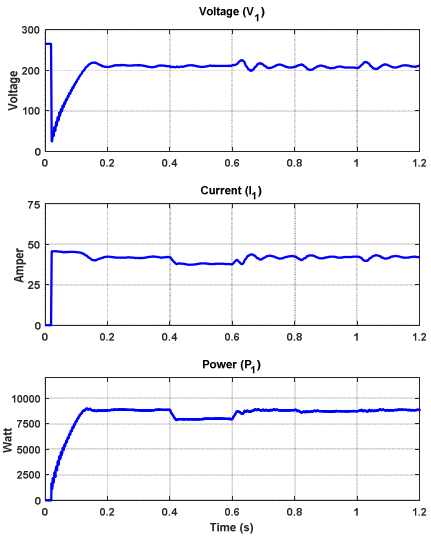

Fig. 6. The PV system output voltage, current and power

The P&O MPPT technique operates in conjunction with a boost dc-dc converter as an interface between a PV system and a HERIC transformerless inverter with a load. The P&O method tracks maximum power point by perturbing the PV voltage and inducing the PV power changes.

Until t=0.4s there are not any variation on irradiance, temperature and load conditions so that it is expected to observe

minimum change on the PV voltage and current and generated power as shown in Figs. 5 and 6. Between t=0.4s and t=0.6s, only the solar irradiance condition changes, and its values is less than before and it is 900 W/m^2 as shown in Fig. 5. The variation of the irradiance have big influence on the short-circuit current and small influence on the open-circuit voltage of a PV module [17]. Therefore, reduction in irradiance causes more specifically decrease on the PV current and power as shown in Fig. 6.

The ambient temperature increases and it is 28^{o}C between t=0.8s and t=1.0s as shown in Fig. 5. An increasing temperature at constant irradiance causes a reduction of open-circuit voltage and output power of a PV array dominantly [17]. The variation of temperature on the PV outputs is not as influential as the irradiance is as shown in Fig. 6.

Fig. 7 shows a reflection of the P&O MPPT technique on the dc-dc converter output. The technique controls the switch of dc-dc converter for maximizing the energy harvest performance and patterns of the dc-dc converter output waveforms is similar to the PV output as shown in Fig. 7.

Between t=0.4s and t=0.6s, variation of irradiance causes decrease in current, voltage and power output as shown in Fig. 5, thereby this situation results in change of the operation point of PV converter's MPPT and shifting to left side. The dc-dc boost converter output voltage and current decrease according to previous time interval as shown in Fig. 7.

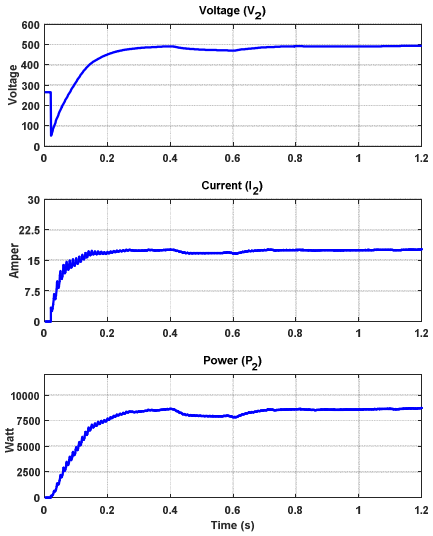

Fig. 7. The dc-dc converter output voltage, current and power

While the dc-dc boost converter is used to extract maximum power from the PV part, the HERIC transformerless inverter is carried out to feed the load. The HERIC inverter is controlled to keep a voltage on reference value by changing of duty cycle of switches of the HERIC inverter.

Due to structure of the HERIC inverter, it is not feasible in case of a voltage sag as shown in Fig. 8. Since the boost dc-dc converter focuses on maximization of power extraction of the PV array, output voltage of the dc-dc power converter can be dropped and effects the HERIC inverter output voltage as shown on Fig. 8.

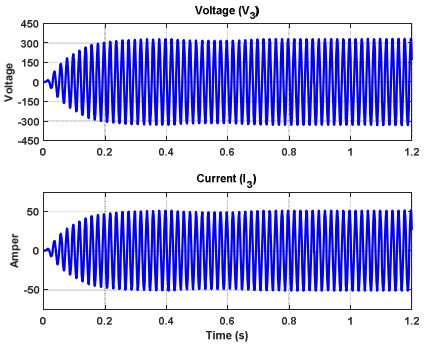

Fig. 8. The load voltage and current waveform

4. Conclusion

In this study, design and simulation of a standalone photovoltaic MPPT system with transformerless inverter are realized. The photovoltaic system is managed by Perturb and Observe (P&O) MPPT technique with dc-dc boost converter for variation in ambient temperature and irradiation. HERIC inverter is controlled by the classical PI controller to supply the load demand (voltage and power). It is observed that the variation of irradiance has more influence on the PV output characteristics than the variation of temperature. While the HERIC inverter control is based on voltage source structure, the maximum power extraction is a main objective for the dc-dc boost converter.

5. References

[1] R. Hejeejo, J. Qiu, T. S. Brinsmead, L. J. Reedman, "Sustainable energy system planning for the management of MGs: a case study in New South Wales, Australia", *IET Renew Power Gen*, vol. 11, no. 2, pp: 228-238, Apr., 2017.

[2] Renewables 2017: Global status report, REN21, 2016, ISBN 978-3-9818107-6-9.

[3] F. Rong, X. Gong, S. Huang, "A novel grid-connected PV system based on MMC to get the maximum power under partial shading conditions", *IEEE Trans. Power Electron.*, vol. 32, no. 6, pp: 4320-4333, Jun., 2017.

[4] M. J. Khan, L. Mathew, "Different kinds of maximum power point tracking control method for photovoltaic systems: A review", *Arch. Computat. Methods Eng*, vol. 1, no. 1, pp: 1-13, Sept., 2016.

[5] H. D. Tafti, A. I. Maswood, G. Konstantinou, J. Pou, F. Blaabjerg, "A general constant power generation algorithm for photovoltaic systems", *IEEE Trans. Power Electron.*, vol. PP, no. 99, pp: 1-1, Jul., 2017.

[6] S. T. Kok, M. Saad, "A reduced leakage current transformerless photovoltaic inverter", *Renew. Energy*, vol. 86, pp: 1103-1112, Feb., 2016.

[7] S. V. Araujo, P. Zacharias, R. Mallwitz, "Highly efficient single-phase transformerless inverters for grid-connected photovoltaic systems", *IEEE Trans. Ind. Electron.*, vol. 57, no. 9, pp: 3118-3128, Sept., 2010.

[8] M. Islam, S. Mekhilef, M. Hasan, "Single phase transformerless inverter topologies for grid-tied photovoltaic system: A review", *Renew. Sustainable Energy Rev.*, vol. 45, pp: 69-86, May., 2015.

[9] W. Li, Y. Gu, H. Luo, W. Cui, X. He, C. Xia, "Topology review and derivation methodology of single-phase transformerless photovoltaic inverters for leakage current

suppression", *IEEE Trans. Ind. Electron.*, vol. 62, no. 7, pp: 4537-4551, Jul., 2015.

[10] D. Barater, E. Lorenzani, C. Concari, G. Franceschini, G. Buticchi, "Recent advances in single-phase transformerless photovoltaic inverters", *IET Renew. Power Gen.*, vol. 10, no. 2, pp: 260-273, Feb., 2016.

[11] F. Blaabjerg, R. Teodorescu, M. Liserre, A. V. Timbus, "Overview of control and grid synchronization for distributed power generation systems", *IEEE Trans. Ind. Electron.,* vol. 53, no. 5, pp: 1398-1409, Oct., 2016.

[12] L. Zhang, K. Sun, Y. Xing, M. Xing, "H6 transformerless full-bridge PV grid-tied inverters", *IEEE Trans. Power Electron.*, vol. 29, no. 3, pp: 1229-1238, Marc., 2014.

[13] Y. Yang, F. Blaabjerg, H. Wang, "Low-voltage ride-through of single-phase transformerless photovoltaic inverters", *IEEE Trans. Ind. Appl.*, vol. 50, no. 3, pp: 1942-1952, May.-Jun., 2014.

[14] W. Sun, Z. Chen, X. Wu, "Intelligent optimize design of LCL filter for three-phase voltage-source PWM rectifier", in *IEEE 6th International Power Electronics and Motion Control Conference 2009 (IPEMC '09)*, Wuhan, China, 2009, pp. 970-974.

[15] S. Saridakis, E. Koutroulis, F. Blaabjerg, "Optimization of SiC-based H5 and Conergy-NPC transformerless PV inverters", *IEEE Trans. Emerg. Sel. Topics Power Electron.*, vol. 3, no. 2, pp: 555-567, Jun., 2015.

[16] A. Reznik, M. G. Simoes, A. Al-Durra, S. M. Muyeen, "LCL filter design and performance analysis for grid-interconnected systems", *IEEE Trans. Ind. Appl.*, vol. 50, no. 2, pp: 1225-1232, Marc.-Apr., 2014.

[17] E. Ozkop, I. H. Altas, "A virtual PV systems lab for engineering undergraduate curriculum", *Int. J. Photoenergy*, vol. 2014, pp: 1-17, 2014.